Experimental Hematology

Experimental Hematology 2019;76:24–37

ORIGINAL ARTICLE

Bmi1 restricts the adipogenic differentiation of bone marrow stromal cells to maintain the integrity of the hematopoietic stem cell niche

Yuko Kato[a,b,c,1], Li-Bo Hou[a,1], Satoru Miyagi[a,b], Eriko Nitta[a,d], Kazumasa Aoyama[a], Daisuke Shinoda[a,e], Satoshi Yamazaki[f], Wakako Kuribayashi[a,e], Yusuke Isshiki[a], Shuhei Koide[a,e], Sha Si[a], Atsunori Saraya[a], Yumi Matsuzaki[b,c], Maarten van Lohuizen[g,h], and Atsushi Iwama[a,e]

[a]*Department of Cellular and Molecular Medicine, Graduate School of Medicine, Chiba University, Chiba, Japan;* [b]*Department of Life Science, Faculty of Medicine, Shimane University, Izumo City, Shimane, Japan;* [c]*PuREC Company, Ltd., Izumo City, Shimane, Japan;* [d]*Division of Structural Medicine, Department of Physiology and Cell Biology, Kobe University Graduate School of Medicine, Hyogo, Japan;* [e]*Division of Stem Cell and Molecular Medicine, Institute of Medical Science, University of Tokyo, Tokyo, Japan;* [f]*Division of Stem Cell Biology, Center for Stem Cell Biology and Regenerative Medicine, Institute of Medical Science, University of Tokyo, Tokyo, Japan;* [g]*Division of Molecular Genetics, The Netherlands Cancer Institute, Amsterdam, The Netherlands;* [h]*Oncode Institute, Amsterdam, The Netherlands*

(Received 27 July 2019; accepted 30 July 2019)

The polycomb group protein Bmi1 maintains hematopoietic stem cell (HSC) functions. We previously reported that *Bmi1*-deficient mice exhibited progressive fatty changes in bone marrow (BM). A large portion of HSCs reside in the perivascular niche created partly by endothelial cells and leptin receptor$^+$ (LepR$^+$) BM stromal cells. To clarify how Bmi1 regulates the HSC niche, we specifically deleted *Bmi1* in LepR$^+$ cells in mice. The *Bmi1* deletion promoted the adipogenic differentiation of LepR$^+$ stromal cells and caused progressive fatty changes in the BM of limb bones with age, resulting in reductions in the numbers of HSCs and progenitors in BM and enhanced extramedullary hematopoiesis. This adipogenic change was also evident during BM regeneration after irradiation. Several adipogenic regulator genes appeared to be regulated by Bmi1. Our results indicate that Bmi1 keeps the adipogenic differentiation program repressed in BM stromal cells to maintain the integrity of the HSC niche.

Hematopoietic stem cells (HSCs) self-renew and differentiate into all blood types, thereby sustaining hematopoiesis during life. HSC niches are specialized bone marrow (BM) microenvironments that maintain HSCs and regulate their functions. The location of HSCs in BM remains controversial; however, recent studies using BM imaging revealed that most HSCs reside adjacent to sinusoidal blood vessels, arterioles, and transition zone vessels, suggesting that HSCs are maintained mostly in the perivascular niche [1–5]. CXC-chemokine ligand 12 (CXCL12) is one of the critical niche factors required for maintaining HSCs [6]. Perivascular stromal cells expressing high levels of CXCL12 have been characterized as CXCL12-abundant reticular (CAR) cells) [6]. On the other hand, the vast majority of perivascular stromal cells, which express SCF and CXCL12, may be identified as leptin receptor-expressing cells (LepR$^+$ cells) [7]. CAR cells and LepR$^+$ cells are considered to represent very similar cell populations. Functionally, LepR$^+$ cell-derived SCF and CXCL12 are required for maintaining HSC pool sizes and mobilization, respectively [8–10]. LepR$^+$ cells, which include skeletal stem cells (SSCs), give

Y.K. and L.B.H. performed experiments, analyzed results, made figures, and actively wrote the article. S.M., E.N., A.K., D.S., S.Y., W.K., Y.I., S.K., S.S., A.S., and Y.M. assisted with experiments. M. v.L. generated mice. A.I. conceived of and directed the study, secured funding, and actively wrote the article.

Offprint requests to: Atsushi Iwama, MD, PhD, Division of Stem Cell and Molecular Medicine, Center for Stem Cell Biology and Regenerative Medicine, Institute of Medical Science, University of Tokyo, 4-6-1 Shirokanedai, Minato-ku, Tokyo, 108-8639 Japan; E-mail: 03aiwama@ims.u-tokyo.ac.jp

[1]YK and LBH contributed equally to this work.

Supplementary material associated with this article can be found in the online version at https://doi.org/10.1016/j.exphem.2019.07.006.

0301-472X/
https://doi.org/10.1016/j.exphem.2019.07.006

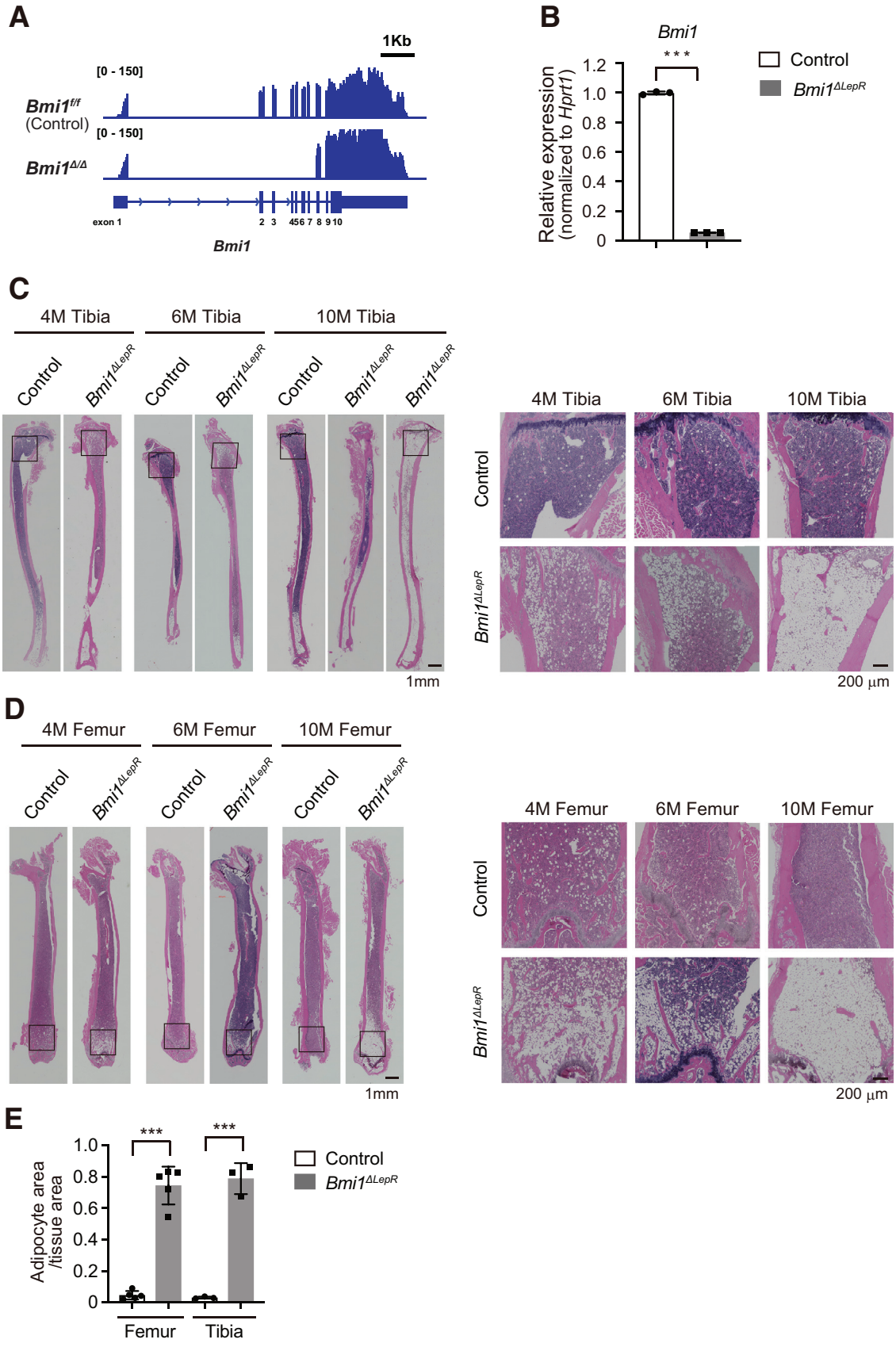
A
1Kb
[0 - 150]
Bmi1f/f
(Control)
[0 - 150]
Bmi1Δ/Δ
exon 1
2 3
456 7 8 9 10
Bmi1
B
Bmi1
***
Relative expression
(normalized to Hprt1)
1.2
1.0
0.8
0.6
0.4
0.2
0
Control
Bmi1ΔLepR
C
4M Tibia
6M Tibia
10M Tibia
Control
Bmi1ΔLepR
1mm
200 μm
D
4M Femur
6M Femur
10M Femur
1mm
200 μm
E
***
***
Adipocyte area
/tissue area
1.0
0.8
0.6
0.4
0.2
0
Femur
Tibia

rise to the majority of bone and adipocytes formed in BM [7,11]. The accumulation of adipocytes in BM progresses with aging, particularly in humans, and has been proposed to cause dysfunctions in BM microenvironments, thereby compromising hematopoiesis [12,13].

Polycomb-group (PcG) proteins form multiprotein complexes that play a key role in the initiation and maintenance of gene silencing through histone modifications [14,15]. Canonical polycomb repressive complex 1 (PRC1) and PRC2 have been characterized in detail, and they exhibit catalytic activities that are specific to the mono-ubiquitination of histone H2A at lysine 119 (H2AK119ub1) and the mono-, di-, and trimethylation of H3 at lysine 27 (H3K27me1/2/3), respectively. After the recruitment of PRC2 to chromatin, PRC2 trimethylates H3K27 (H3K27me3), which, in turn, recruits canonical PRC1 via the CBX subunit that binds to H3K27me3. We and others previously reported that *Bmi1/Pcgf4*, a core component of PRC1, is cell-autonomously required for the self-renewal of HSCs by transcriptionally repressing the *Cdkn2a* locus [16–18]. We also found that $Bmi1^{\Delta/\Delta}$ BM exhibited progressive fatty changes and failed to support the reconstitution of HSCs, indicating a role for Bmi1 in the regulation of the HSC niche. Based on these findings, we hypothesized that *Bmi1* regulates self-renewing HSCs in cell-autonomous and non–cell-autonomous manners. However, the niche cells that require Bmi1 to support HSC functions have not yet been identified, and the mechanisms by which Bmi1 regulates HSC niche cells remain unclear.

In the present study, we generated a mouse line in which *Bmi1* was specifically deleted in $LepR^+$ BM stromal cells (BMSCs) ($Bmi1^{fl/fl}$*; LepR-Cre*) and found that the *Bmi1* deletion promoted the adipogenic differentiation of $LepR^+$ BMSCs in BM and reduced the HSC pool size moderately. Expression profiling and ChIP sequences of the PRC1 mark, H2AK119ub1, identified regulators of adipogenesis, such as *Nf2f2* and *Hox* family genes, as direct downstream targets of Bmi1. The present results provide a novel function for Bmi1 in the maintenance of HSCs.

Methods

Mice

The conditional *Bmi1* allele ($Bmi1^{fl}$), which contains LoxP sites flanking *Bmi1* exons 2 and 7, was generated. *LepR-Cre* mice were purchased from the Jackson Laboratory and backcrossed at least six times onto a C57BL/6 (CD45.2) background. $Bmi1^{fl/fl}$ mice were crossed with *LepR-Cre* mice (JAX Lab, Bar Harbor, ME, No. 008320) to achieve the conditional deletion of *Bmi1*. C57BL/6 mice congenic for the Ly5 locus (CD45.1) were purchased from Sankyo-Lab Service (Tsukuba, Japan). Age-matched female pairs were analyzed in each experiment unless otherwise specified in the figure legends. All experiments using mice were performed in accordance with our institutional guidelines for the use of laboratory animals and approved by the Review Board for Animal Experiments of Chiba University (Approval ID: 30-56).

Statistical analysis

Statistical tests were performed using Graph Pad Prism Version 6. The significance of differences was measured with Student's *t* test. Data are expressed as the mean ± SD. Significance was taken at values of $p < 0.05$, $p < 0.01$, and $p < 0.001$.

Deposition of data

RNA sequence and ChIP sequence data were deposited in the DNA Data Bank of Japan (DDBJ) (Accession No. DRA007413).

Results

Deletion of Bmi1 *in* $LepR^+$ *BMSCs promotes adipogenic differentiation*

To clarify the role of Bmi1 in niche cells, we generated a mouse line in which *Bmi1* exons 2 to 7 were specifically deleted in leptin receptor$^+$ ($LepR^+$) BMSCs ($Bmi1^{fl/fl}$*; LepR-Cre*). We confirmed the efficient deletion of *Bmi1* in $LepR^+$ cells by an RNA sequence analysis (Figure 1A) and real-time reverse transcription quantitative polymerase chain reaction (RT-qPCR) (Figure 1B). In contrast, *Bmi1* expression in HSCs was not changed in 3-month-old $Bmi1^{\Delta LepR}$ mice compared with control mice (control 18.8 vs. $Bmi1^{\Delta LepR}$ 20.9 reads per kilobase of exons per million mapped reads [RPKM]). We hereafter refer to *LepR-Cre;* $Bmi1^{fl/fl}$ mice as $Bmi1^{\Delta LepR}$ mice. We used $Bmi1^{fl/fl}$ mice as controls and confirmed that their BM phenotypes were almost identical to those of $Bmi1^{wt/wt}$*; LepR-Cre* mice (Supplementary Figure E1A, online only, available at www.exphem.org). $Bmi1^{\Delta LepR}$ mice were born and grew healthy. Cre activity has also been detected in the hypothalamus, limbic and cortical brain regions, and retrosplenial cortex in *LepR-Cre* mice. Although

Figure 1. Deletion of *Bmi1* in $LepR^+$ stromal cells promotes adipogenic differentiation. **(A)** Snapshots of RNA-seq signals at the *Bmi1* gene locus in control and $Bmi1^{\Delta LepR}$ BM $LepR^+$ stromal cells. **(B)** A quantitative RT-PCR analysis of *Bmi1* expression in control and $Bmi1^{\Delta LepR}$ $LepR^+$ cells from 6-month-old mice. mRNA levels were normalized to *Hprt1* expression, and relative expression levels are expressed as the mean ± SD of triplicate analyses. ***$p < 0.001$ by Student's *t* test. **(C, D)** Hematoxylin and eosin staining of sections of decalcified tibias **(C)** and femurs **(D)** from 4-, 6-, and 10-month-old mice. Images with the higher magnifications of boxed areas are depicted in the right panels. Bars = 1 mm and 200 μm, respectively. **(E)** Adipocyte areas at epiphysis of tibias and femurs from 10-month-old mice boxed in **(C)** and **(D)** were quantified by analyzing images of bone sections stained with hematoxylin and eosin using the software ImageJ and are shown relative to total tissue areas. Data are expressed as the mean ± SD. ***$p < 0.001$ by Student's *t* test.

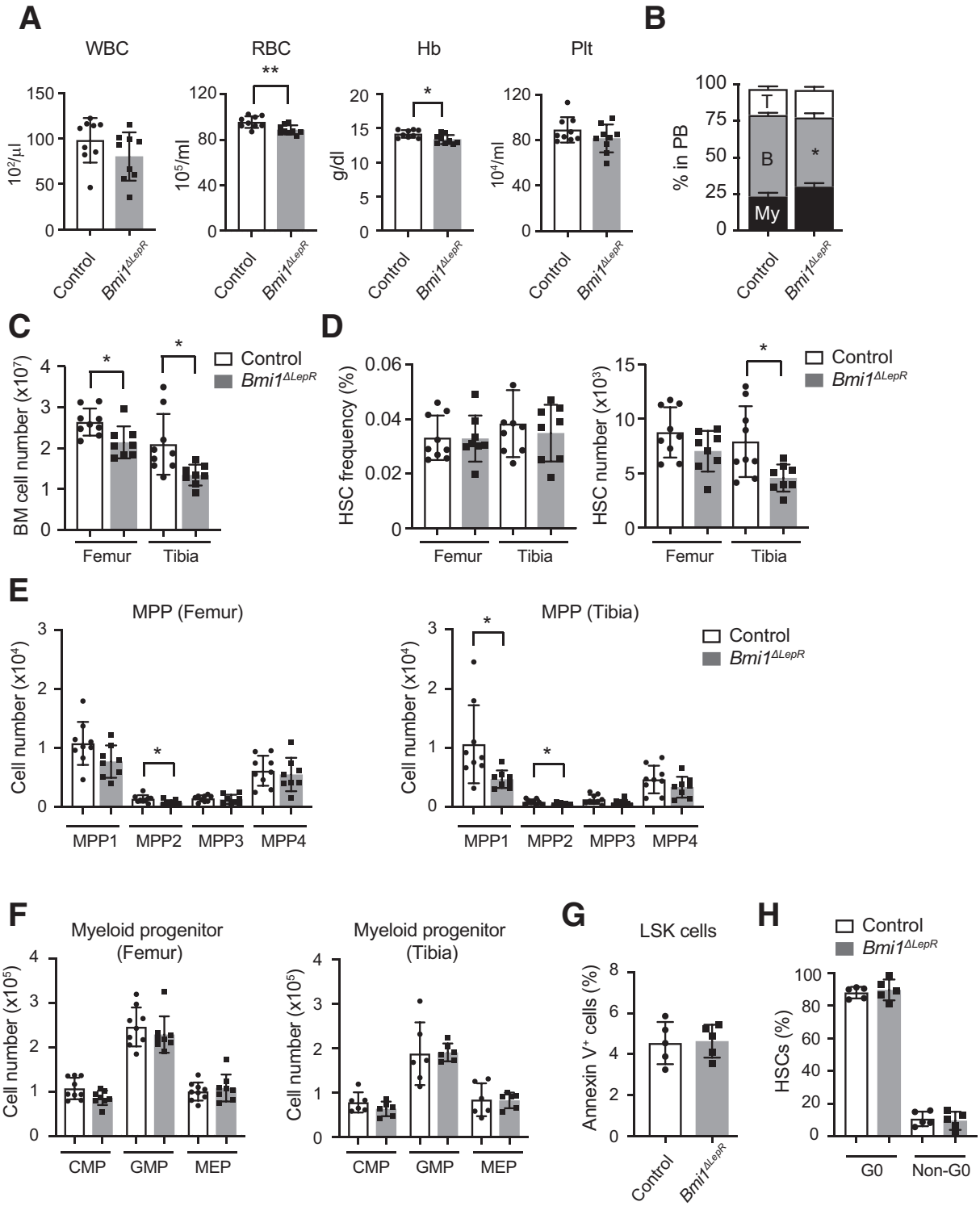

Figure 2. Reduction in the HSC pool size in *Bmi1*$^{\Delta LepR}$ mice. **(A)** White blood cell (WBC), red blood cell (RBC), hemoglobin (Hb), and platelet (PLT) counts in the PB of 11-month-old control and *Bmi1*$^{\Delta LepR}$ mice ($n = 9$). **(B)** Proportions of myeloid cells (My) (Mac-1$^+$ and/or Gr-1$^+$), B220$^+$ B cells, and CD4$^+$ or CD8$^+$ T cells in PB hematopoietic cells ($n = 9$). **(C–F)** Absolute numbers of total BM cells **(C)**, frequency of CD150$^+$CD48$^-$CD34$^-$LSK HSCs and their absolute numbers **(D)**, and absolute numbers of MPPs **(E)** and myeloid progenitors **(F)** in femurs ($n = 8$ or 9) and tibias ($n = 8$ or 9) from 11-month-old control and *Bmi1*$^{\Delta LepR}$ mice. **(G)** Percentages of Annexin V$^+$ cells in LSK HSPCs in tibias and femurs from 10-month-old control and *Bmi1*$^{\Delta LepR}$ mice ($n = 5$). **(H)** Cell cycle status of HSCs in tibias and femurs from 10-month-old control and *Bmi1*$^{\Delta LepR}$ mice detected by Ki67 and 7AAD staining ($n = 5$). Data are expressed as the mean ± SD. The significance of differences is shown relative to the *Bmi1*$^{fl/fl}$ control mice. * $p < 0.05$, ** $p < 0.01$ by Student's t test.

Bmi1$^{\Delta LepR}$ mice did not show obvious abnormalities in behavior and food intake, they had more adipose mass and gained more body weight than control mice with age (Supplementary Figure E1B, C).

We initially analyzed the histology of femurs and tibias from 4-, 6-, and 10-month-old *Bmi1*$^{\Delta LepR}$ mice and found that *Bmi1*$^{\Delta LepR}$ BM exhibited adipogenic changes, which occurred from the epiphysis and gradually progressed to the diaphysis with age (Figure 1C, D). Adipogenic changes were more severe in tibias than in femurs (Figure 1C, D), but were not evident in sternums (Supplementary Figure E2, online only, available at www.exphem.org). Of interest, the frequency of LepR$^+$ BMSCs in sternums was more than fivefold lower than that in long bones (data not shown). Immunostaining of Perilipin, a protein that coats lipid droplets in adipocytes, also revealed accumulation of adipocytes in *Bmi1*$^{\Delta LepR}$ tibia. Conversely, the numbers of CD144/VE-Cadherin$^+$ endothelial cells were reduced in *Bmi1*$^{\Delta LepR}$ tibias compared with the control tibias (Supplementary Figure E3, online only, available at www.exphem.org). These results indicated that the loss of Bmi1 promoted the adipogenic differentiation of LepR$^+$ BMSCs, particularly in long bones.

Reductions in the HSC pool size in Bmi1$^{\Delta LepR}$ *mice*

To examine the effects of adipogenic changes in BM on hematopoiesis in *Bmi1*$^{\Delta LepR}$ mice, we analyzed hematopoiesis in 11-month-old *Bmi1*$^{\Delta LepR}$ mice. These mice exhibited mild anemia and slight reductions in the proportion of B lymphocytes in peripheral blood (PB) (Figure 2A, B). BM cellularity in tibias and femurs was significantly lower in *Bmi1*$^{\Delta LepR}$ mice than in control mice (Figure 2C). Absolute numbers, but not the frequencies of CD150$^+$CD48$^-$CD34$^-$Lin$^-$Sca1$^+$c-Kit$^+$ (LSK) HSCs, were similarly reduced; however, those in the femurs of *Bmi1*$^{\Delta LepR}$ mice were only slightly lower than those in control femurs (Figure 2D). Reductions in the numbers of multipotent progenitors were also more evident in tibias than in femurs from Bmi1$^{\Delta LepR}$ mice than those from control mice, while the numbers of myeloid progenitors did

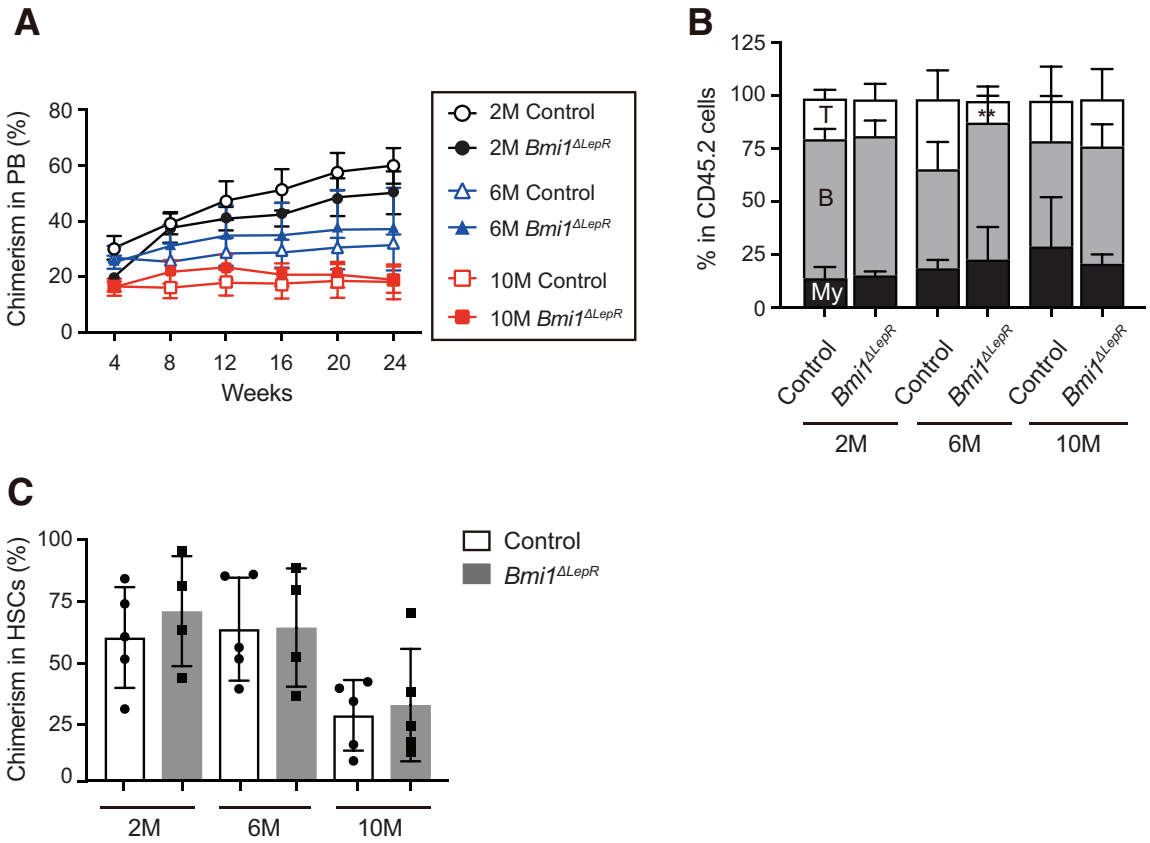

Figure 3. HSCs in *Bmi1*$^{\Delta LepR}$ mice maintain a normal repopulating capacity. **(A)** Competitive repopulating assays using HSCs from *Bmi1*$^{\Delta LepR}$ mice. Sixty CD45.2$^+$ CD150$^+$CD48$^-$CD34$^-$LSK HSCs from 2-, 6-, and 10-month-old control and *Bmi1*$^{\Delta LepR}$ mice were transplanted into lethally irradiated CD45.1$^+$ recipient mice along with 2×10^5 CD45.1$^+$ WT BM cells. The chimerism of CD45.2$^+$ donor cells in the PB are indicated ($n = 4$ or 5). **(B)** The proportions of myeloid (My) (Mac-1$^+$ and/or Gr-1$^+$), B220$^+$ B, and CD4$^+$ or CD8$^+$ T cells in CD45.2$^+$ donor-derived hematopoietic cells in PB 6 months after transplantation ($n = 4$ or 5). **(C)** The chimerism of CD45.2$^+$ donor cells in CD150$^+$CD48$^-$CD34$^-$LSK HSCs ($n = 4$ or 5). Data are expressed as the mean ± SD. The significance of differences is shown relative to the *Bmi1*$^{fl/fl}$ control mice. $^{**}p < 0.01$ by Student's *t* test.

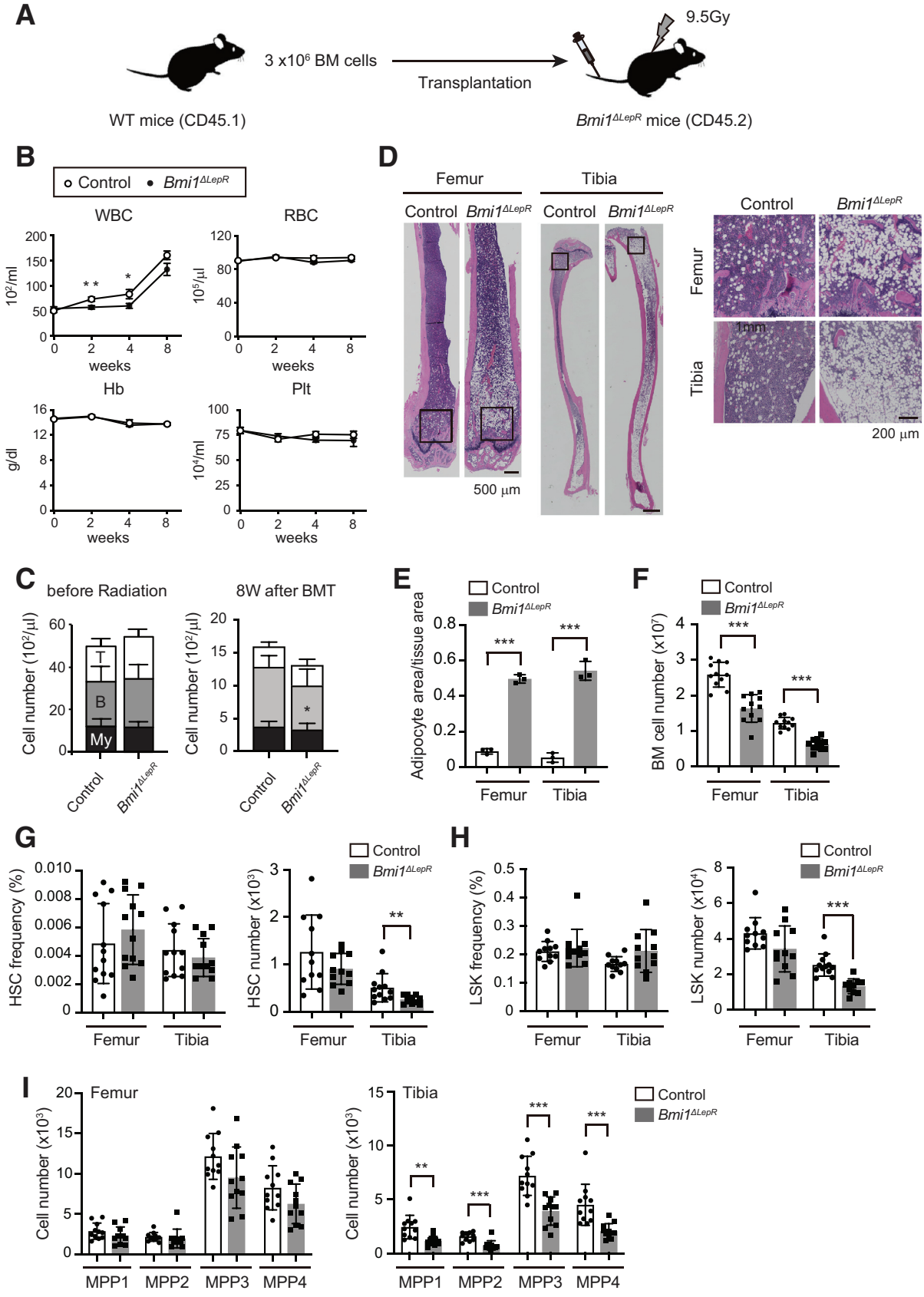
A
9.5Gy
3 x10⁶ BM cells
Transplantation
WT mice (CD45.1)
Bmi1ΔLepR mice (CD45.2)
B
Control
Bmi1ΔLepR
WBC
RBC
Hb
Plt
weeks
D
Femur
Tibia
500 μm
1mm
200 μm
C
before Radiation
8W after BMT
Cell number (10²/μl)
E
Adipocyte area/tissue area
F
BM cell number (x10⁷)
G
HSC frequency (%)
HSC number (x10³)
H
LSK frequency (%)
LSK number (x10⁴)
I
Cell number (x10³)
MPP1
MPP2
MPP3
MPP4

not markedly change in the absence of Bmi1 (Figure 2E, F). Annexin staining of LSK hematopoietic stem and progenitor cells (HSPCs) and Ki67 staining of $CD150^{+}CD48^{-}CD34^{-}$LSK HSCs from 10-month-old mice revealed no significant changes in apoptosis or the cell cycle status between control and $Bmi1^{\Delta LepR}$ mice (Figure 2G, H). Of note, hematopoiesis in 4-month-old $Bmi1^{\Delta LepR}$ mice was largely intact (Supplementary Figure E4, online only, available at www.exphem.org). These results indicated that the fatty change in BM triggered by the loss of Bmi1 in $LepR^{+}$ BMSCs progressed with age and reduced the HSPC pool size moderately.

Despite impaired hematopoiesis in BM, overall hematopoiesis was maintained nearly intact, suggesting compensation by extramedullary hematopoiesis. Spleen and liver from 13-month-old $Bmi1^{\Delta LepR}$ mice were moderately enlarged (Supplementary Figure E5A, online only, available at www.exphem.org), and histological analyses revealed that extramedullary hematopoiesis was active in the spleen, whereas it was minimal in the liver (Supplementary Figure E5B). Flow cytometric analyses of the spleen revealed active myelopoiesis (Supplementary Figure E5C) and a significant increase in the number of LSK HSPCs in the spleen of $Bmi1^{\Delta LepR}$ mice compared with control mice (Supplementary Figure E5D). Myeloid progenitors were also increased, albeit with no statistical significance (Supplementary Figure E5E). We then performed homing assays. We transplanted 5×10^5 WT CD45.1 c-Kit^{+} cells into non-irradiated control and $Bmi1^{\Delta LepR}$ mice and analyzed the presence of LSK cells in femur, tibia, and spleen 4 hours after transplantation. The numbers of LSK cells detected in BM and spleen of young control and $Bmi1^{\Delta LepR}$ recipients (2-month-old) were comparable (Supplementary Figure E6, online only, available at www.exphem.org). In contrast, those of LSK cells detected were significantly lower in BM of 13-month-old $Bmi1^{\Delta LepR}$ recipient mice than in the age-matched control recipient mice (Supplementary Figure E6, online only, available at www.exphem.org). These data indicate that advanced adipogenic changes compromise the homing of HSPCs and cause egression of a portion of HSPCs from BM to other organs to initiate compensatory hematopoiesis.

HSCs in $Bmi1^{\Delta LepR}$ *mice maintain a normal repopulating capacity*

To test the repopulating capacity of HSCs in $Bmi1^{\Delta LepR}$ mice, we performed competitive repopulation assays using 60 $CD45.2^{+}$ HSCs ($CD150^{+}CD48^{-}CD34^{-}$LSK) from the femurs and tibias of 2-, 6-, or 10-month-old $Bmi1^{\Delta LepR}$ mice combined with 2×10^5 competitor BM cells from CD45.1 mice. The capacity of donor HSCs to repopulate PB hematopoietic cells in recipient mice declined with the aging of donor mice; however, HSCs from $Bmi1^{\Delta LepR}$ mice repopulated PB hematopoietic cells, including myeloid, B, and T cells, at levels similar to those from age-matched control mice (Figure 3A, B). Correspondingly, the chimerism of $Bmi1^{\Delta LepR}$ donor cells in HSCs in recipient BM was similar to that of the control (Figure 3C). These results indicated that the loss of Bmi1 affected the HSC pool size, but not HSC function.

We next analyzed the function of progenitor cells. Because the hematopoiesis in 4-month-old young $Bmi1^{\Delta LepR}$ mice was almost intact, we analyzed progenitor cells in 8-week-old mice. We first evaluated the numbers of colony-forming units in tibias and found no significant difference between control and $Bmi1^{\Delta LepR}$ mice (Supplementary Figure E7A, online only, available at www.exphem.org). We next transplanted BM cells from tibias into lethally irradiated recipient mice. BM cells from $Bmi1^{\Delta LepR}$ mice showed normal repopulation capacity of hematopoiesis and repopulated comparable numbers of MPPs and myeloid progenitors to control mice in recipient mice 4 weeks after transplantations (Supplementary Figure E7B–D). These results indicate that progenitor cells in $Bmi1^{\Delta LepR}$ mice are functionally intact.

Hematopoietic regeneration in $Bmi1^{\Delta LepR}$ *mice*

To test the capability of $LepR^{+}$ BMSCs lacking Bmi1 to support the regeneration of the hematopoietic system, BM cells from CD45.1 mice were transplanted into lethally irradiated 8-week-old control or $Bmi1^{\Delta LepR}$ mice (Figure 4A). The loss of Bmi1 in $LepR^{+}$ BMSCs did not have any impact on blood cell counts in 8-week-old recipients before irradiation (0 weeks in Figure 4B).

Figure 4. Hematopoietic regeneration in $Bmi1^{\Delta LepR}$ mice. **(A)** Strategy for the analysis of regeneration after irradiation in $Bmi1^{\Delta LepR}$ mice. CD45.1 BM cells (3×10^6) from wild-type mice were transplanted into lethally irradiated 2-month-old CD45.2 $Bmi1^{fl/fl}$ or $Bmi1^{\Delta LepR}$ mice. **(B)** PB cell counts in nonirradiated mice or at 2, 4, or 8 weeks after irradiation and transplantation ($n = 11$ or 12). **(C)** The absolute numbers of myeloid (My) (Mac-1^{+} and/or Gr-1^{+}), $B220^{+}$ B, and $CD4^{+}$ or $CD8^{+}$ T cells among $CD45.1^{+}$ donor-derived hematopoietic cells in PB from nonirradiated mice or at 8 weeks after irradiation and transplantation ($n = 11$). **(D)** Hematoxylin and eosin staining of sections of decalcified tibias and femurs from recipient mice 8 weeks after irradiation and transplantation. Bars = 200 μm, 500 μm, and 1 mm. **(E)** Adipocyte areas at the epiphysis were quantified by analyzing images of bone sections stained with hematoxylin and eosin using the software ImageJ and are shown relative to total tissue areas. **(F)** Absolute numbers of total BM cells per femur or tibia 8 weeks after irradiation and transplantation ($n = 11$). (G–I) Frequency of $CD150^{+}CD48^{-}CD34^{-}$LSK HSCs **(G)** and LSK cells **(H)** and their absolute numbers, and absolute numbers of MPPs **(I)** per femur or tibia ($n = 11$) from recipient mice 8 weeks after irradiation and transplantation. The significance of differences is shown relative to the $Bmi1^{fl/fl}$ control. Data are expressed as the mean ± SD. The significance of differences is shown relative to the $Bmi1^{fl/fl}$ control mice. * $p < 0.05$, ** $p < 0.01$, *** $p < 0.001$ by Student's t test.

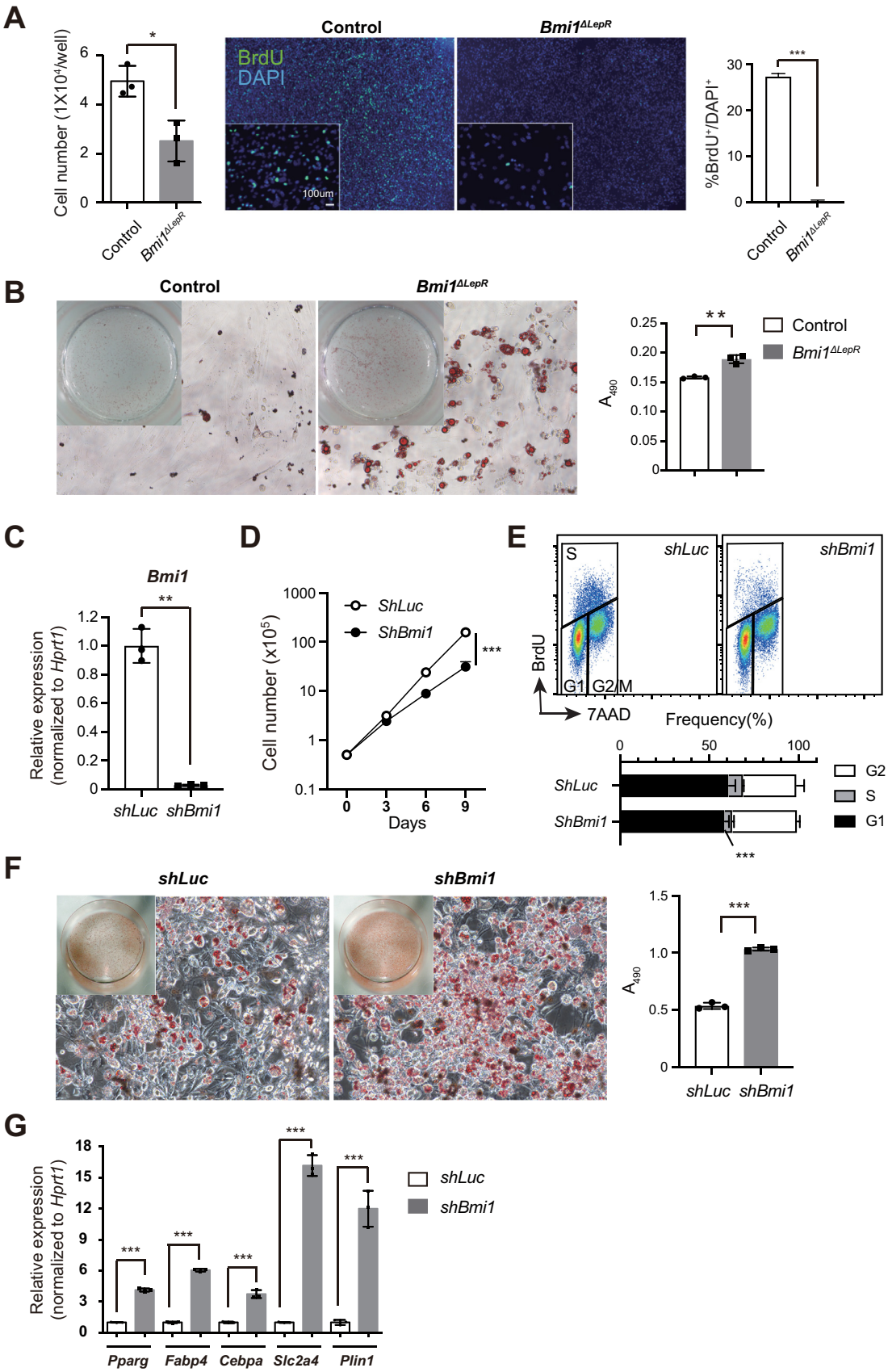
A
Control
Bmi1ΔLepR
BrdU
DAPI
100um
Cell number (1X10⁴/well)
%BrdU⁺/DAPI⁺
B
Control
Bmi1ΔLepR
A490
C
Bmi1
Relative expression (normalized to Hprt1)
shLuc shBmi1
D
ShLuc
ShBmi1
Cell number (x10⁵)
Days
E
S
shLuc
shBmi1
BrdU
7AAD
G1 G2/M
Frequency(%)
G2
S
G1
F
shLuc
shBmi1
G
Relative expression (normalized to Hprt1)
Pparg Fabp4 Cebpa Slc2a4 Plin1

Bmi1$^{\Delta LepR}$ recipients showed delayed recovery of WBC counts (Figure 4B) and mild, but significantly greater reductions in the percentages of B cells in PB than control recipients (Figure 4C), although these phenotypes were largely attenuated 20 weeks after transplantation (Supplementary Figure E8, online only, available at www.exphem.org). BM analyses also revealed greater reductions in BM cellularity in *Bmi1*$^{\Delta LepR}$ recipients than in control recipients 8 weeks after transplantation because of advanced fatty changes in tibias and femurs (Figure 4D–F). Accordingly, BM analyses revealed greater reductions in the numbers of HSCs, LSK HSPCs, and multipotent progenitors (MPPs) in *Bmi1*$^{\Delta LepR}$ recipients than in control recipients, with the reductions observed in tibias, but not in femurs, being significant (Figure 4G–I). These results indicated that irradiation promoted the adipogenic differentiation of LepR$^+$ stromal cells and that Bmi1 was required for LepR$^+$ stromal cells to fully support hematopoietic regeneration in the setting of transplantation following myeloablative preconditioning, such as irradiation. In this study, we transplanted 3×10^6 viable total BM cells, which included CD150$^+$CD48$^-$CD34$^-$LSK HSCs, LepR$^+$ BMSCs, and PDGFRα^+CD31$^-$CD45$^-$Ter119$^-$ BMSCs at the frequencies of 0.002%, 0.01%, and 0.2%, respectively. It is possible that WT BMSCs included in donor BM cells engrafted and ameliorated the adipogenic changes of *Bmi1*$^{\Delta LepR}$ recipient mice to some extent.

Bmi1 restricts the adipogenic differentiation of stromal cells

To test whether Bmi1 regulates the adipogenic differentiation of BMSCs in a cell-autonomous manner, we purified control and *Bmi1*$^{\Delta LepR}$ LepR$^+$ BMSCs (CD45$^-$Ter119$^-$Lepr$^+$Sca1$^-$CD31$^-$) (Supplementary Figure E9A, online only, available at www.exphem.org). LepR$^+$ BMSCs expressed *Cxcl12, Kitl*, and *Foxc1* as reported [10,19], but not endothelial cell genes, such as *Endomucin* and *Tie2*. LepR$^+$ BMSCs also expressed osteoblastic genes such as *Osterix* as recently reported [20] (Supplementary Figure E9B). We then cultured these cells. Of note, *Bmi1*$^{\Delta LepR}$ LepR$^+$ cells proliferated poorly in maintenance medium while control cells did (Figure 5A). Interestingly, *Bmi1*$^{\Delta LepR}$ LepR$^+$ cells showed enhanced adipogenic differentiation compared with control cells under adipogenic differentiation conditions (Figure 5B).

We next tested the mouse fibroblast cell line, 3T3-L1, which has the potential to differentiate into adipocytes [21]. We depleted *Bmi1* in 3T3-L1 cells by infecting them with shRNAs against a *Luciferase* (*Luc*) control or *Bmi1* (Figure 5C). Knockdown cells were first cultured in maintenance medium. Cell growth of *Bmi1* knockdown cells was mildly but significantly impaired compared with that of control cells (Figure 5D, E). We then cultured them for 10 days in adipocyte differentiation medium. Oil Red O staining revealed significantly higher levels of lipid accumulation in *Bmi1*-depleted cells than in the control cells, as evaluated by microscopically representative fields and the absorbance of the dye extracted from these cells (Figure 5F). Furthermore, the expression of adipocyte marker genes, such as *Pparg* and *Cebpa*, was induced in *Bmi1*-depleted cells (Figure 5G). These results clearly showed that the inhibition of Bmi1 promoted the adipocyte differentiation of BMSCs.

Profiling of target genes of Bmi1 in BMSCs

Bmi1 is a core component of PRC1, which negatively regulates gene expression by adding H2AK119ub1 at the promoters of its target genes. To elucidate the molecular mechanisms underlying the adipogenic differentiation of BMSCs induced by the loss of Bmi1, chromatin immunoprecipitation DNA sequencing (ChIP-seq) for H2AK119ub1 was performed using BM LepR$^+$ BMSCs purified from

Figure 5. Bmi1 restricts the adipocyte differentiation of BMSCs. **(A)** Growth of *Bmi1*$^{\Delta LepR}$ LepR$^+$ BMSCs. Control and *Bmi1*$^{\Delta LepR}$ LepR$^+$ BMSCs (CD45$^-$Ter119$^-$Lepr$^+$Sca1$^-$CD31$^-$) were sorted from 8-week-old mice and cultured in maintenance medium for 10 days. Cell numbers per well of 96 microtiter plates at day 10 of culture are depicted (*left panel*). The cells were then labeled with 10 μmol/L BrdU for 24 hours and stained with anti-BrdU antibody and DAPI. Microscopic images of BrdU and DAPI are depicted in the middle panels. The proportions of BrdU$^+$DAPI$^+$ cells are depicted in the right panel. Data are expressed as the mean ± SD of triplicate cultures. **(B)** Adipogenic differentiation of LepR$^+$ BMSCs. Control and *Bmi1*$^{\Delta LepR}$ LepR$^+$ BMSCs were cultured for 11 days under adipogenic differentiation conditions. Cells were stained with Oil Red O. Microscopic images are depicted in the left panels. The absorbance of the dye extracted from cells is shown in the right panels. Data are expressed as the mean ± SD of triplicate cultures. **(C)** Knockdown efficiencies evaluated by detecting *Bmi1* mRNA expression by RT-qPCR analysis. 3T3-L1 preadipocytes were infected with lentiviruses expressing shRNA against either *luciferase* (*Luc*; control) or *Bmi1*, and GFP-positive cells were then sorted by flow cytometry 48 hours after transduction. Data are expressed as the mean ± SD of triplicate analyses. **(D)** Growth of *Bmi1* knockdown 3T3-L1 cells. Sorted cells were cultured in maintenance medium, counted, and replated every 3–4 days in triplicates. **(E)** Cell cycle of *Bmi1* knockdown 3T3-L1 cells. Growing cells were labeled with 10 μmol/L BrdU for 3 hours and stained with anti-BrdU antibody and 7-AAD. Representative flow cytometric profiles are depicted in the upper panel. Cell cycle distribution is shown in the lower panel. Data are expressed as the mean ± SD of triplicate analyses. **(F)** Adipocyte differentiation of *Bmi1* knockdown 3T3-L1 cells. Sorted cells were cultured in medium with an adipogenic cocktail. Cells were stained with Oil Red O. Microscopic images are depicted in the left panels. The absorbance of the dye extracted from cells on day 10 of the culture is shown in the right panels. Data are expressed as the mean ± SD of triplicate cultures. **(G)** Expression of adipogenic regulator genes in *Bmi1* knockdown 3T3-L1 cells. Sorted cells were cultured in medium with an adipogenic cocktail. On day 4 of the culture, the expression of adipogenic regulator genes was examined by RT-qPCR. All mRNA levels were normalized to *Hprt1* expression, and relative expression levels are expressed as the mean ± SD of triplicate analyses. *$p < 0.05$, *$p < 0.01$, ***$p < 0.001$ by Student's *t* test.

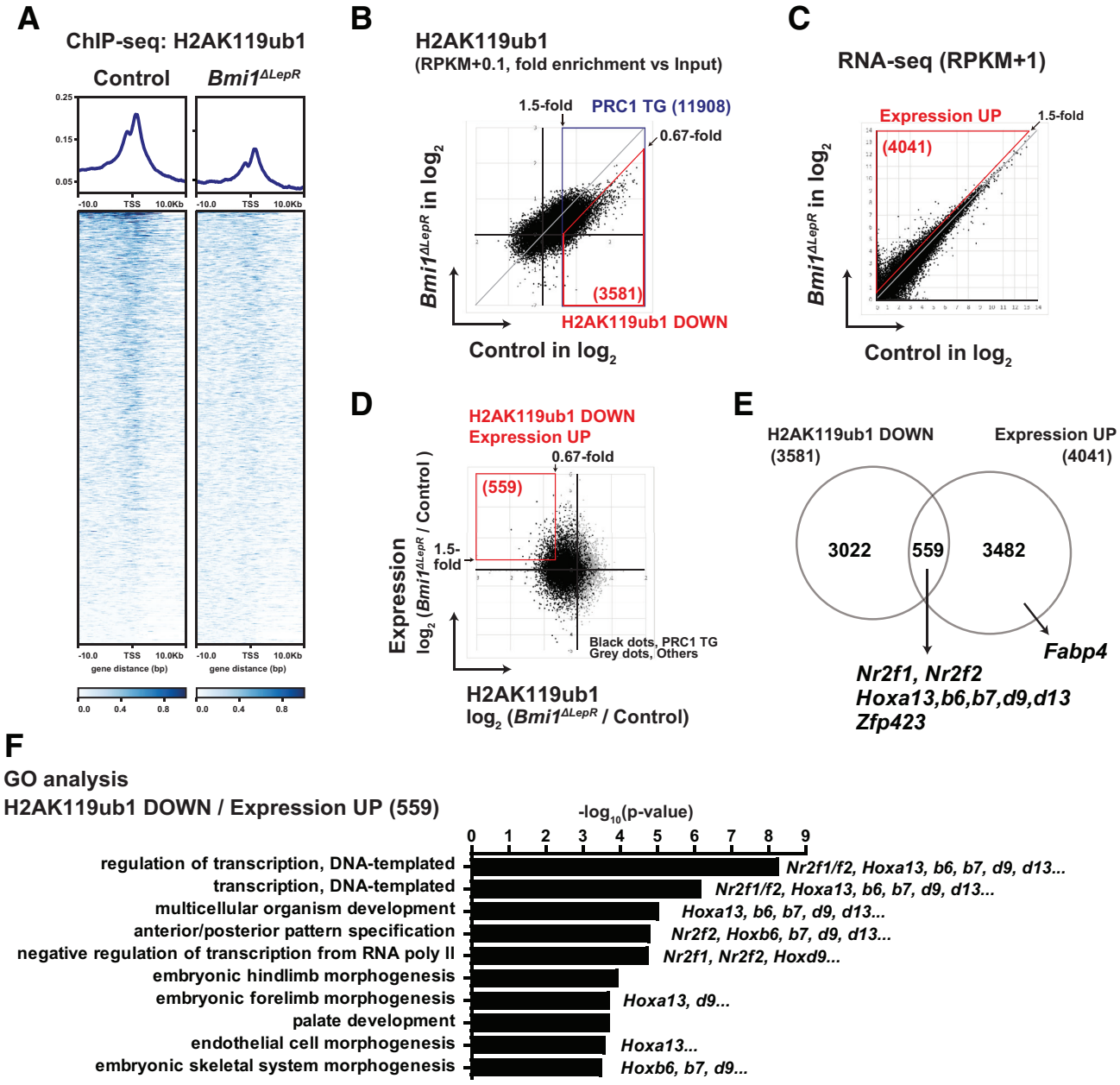

Figure 6. Profiling of target genes of Bmi1 in BM stromal cells. **(A)** Heatmap showing H2AK119ub1 levels around the TSS (TSS ± 10.0 kb) in control and *Bmi1*$^{\Delta LepR}$ BM LepR^{+} cells from 2-month-old male mice. **(B)** Scatterplots revealing the relationship of the fold enrichment values of H2AK119ub1 ChIP signals against the input signals (ChIP/input) at TSS ± 2.0 kb of RefSeq genes (listed in RefSeq ID) between control and *Bmi1*$^{\Delta LepR}$ BM LepR^{+} cells. **(C)** Scatterplots revealing the relationship of expression levels represented as RPKM+1 between control and *Bmi1*$^{\Delta LepR}$ BM LepR^{+} cells from 6-month-old mice. **(D)** A scatterplot revealing the relationship between the levels of H2AK119ub1 and gene expression in control versus *Bmi1*$^{\Delta LepR}$ BM LepR^{+} cells. **(E)** Venn diagram comparing the overlap between genes exhibiting the reductions in H2AK119ub1 levels and those exhibiting its upregulation in *Bmi1*$^{\Delta LepR}$ BMSCs compared with the control BMSCs. **(F)** Gene ontology analysis of overlapped genes in **(E)** using DAVID Bioinformatics Resources. The top 10 GO terms and their *p* values are shown.

control and *Bmi1*$^{\Delta LepR}$ mice. A heatmap showed that H2AK119ub1 levels around the transcription start site (TSS) were moderately reduced by the *Bmi1* deletion (Figure 6A). We then calculated the enrichment of H2AK119ub1 ChIP signals over input signals at the promoter region (TSS ± 2.0 kb) of RefSeq genes and assessed the relationship between control and *Bmi1*$^{\Delta LepR}$ cells (Figure 6B). We defined the 11,908 genes that exhibited more than a 1.5-fold enrichment in H2AK119ub1 signals in WT cells as PRC1 target genes (PRC1 TG). Among PRC1 TG, 3,581 genes showed reductions in H2AK119ub1 levels of >1.5-fold by the loss of Bmi1. RNA sequencing (RNA-seq) revealed that the expression levels of 4,041 genes were upregulated by >1.5-fold in the number of

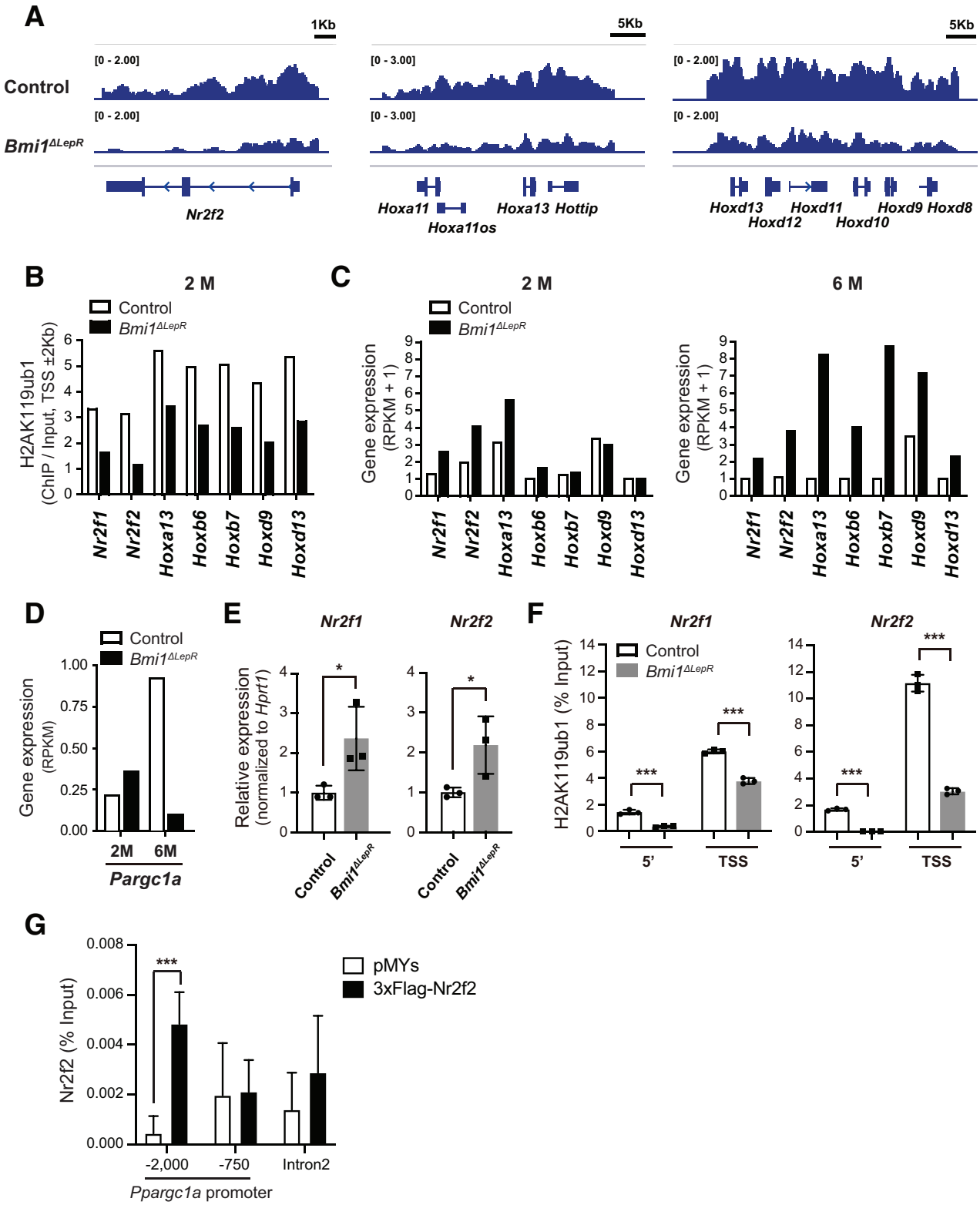

Figure 7. Validation of Bmi1 target genes in BM stromal cells. **(A)** Snapshots of the ChIP-seq signals of H2AK119ub1 at the *Nr2f2* gene, *Hoxa* locus, and *Hoxd* locus in control and *Bmi1*$^{\Delta LepR}$ BM LepR^{+} cells from 2-month-old male mice. The structures of each gene locus including relevant exons are indicated at the bottom of each related snapshot. **(B)** Bar graphs showing H2AK119ub1 levels at the promoters (TSS ± 2.0 kb) of the indicated genes. **(C, D)** Bar graphs showing the gene expression levels of the indicated genes in control and *Bmi1*$^{\Delta LepR}$ BM LepR^{+} cells from 2- and 6-month-old mice. **(E)** Quantitative RT-PCR analysis of control and *Bmi1*$^{\Delta LepR}$ BM LepR^{+} cells from 6-month-old mice. mRNA levels were normalized to *Hprt1* expression, and relative expression levels are expressed as the mean ± SD of triplicate analyses. **(F)** ChIP

RPKM (Figure 6C). To identify the direct target of Bmi1 responsible for aberrant adipogenesis in *Bmi1*$^{\Delta LepR}$ BMSCs, we focused on the 559 genes that displayed both the downregulation of H2AK119ub1 (<0.67-fold) and the upregulation of gene expression upon the *Bmi1* deletion (>1.5-fold) (Figure 6D, E). The expression of mature adipocyte marker genes, such as *Ppargc1, Cebpa, Slc2a4*, and *Plin1*, was not upregulated in *Bmi1*-deficient LepR$^+$ cells. In contrast, several pre-adipocyte genes, such as *Fabp4* and *Zfp423*, were upregulated (Figure 6E; Supplementary Table E1, online only, available at www.exphem.org), suggesting that LepR$^+$ BMSCs are primed for adipogenesis in the absence of Bmi1. On the other hand, a gene ontology (GO) analysis of the 559 potential Bmi1 target genes showed that they were enriched in genes associated with transcription or development, including *Nr2f2* (also known as *Coup-TfII*) and *Hox* family genes (Figure 6F).

Nr2f and *Hox* family genes have been implicated in the transcriptional regulation of adipocyte differentiation [22–24]. They showed reductions in H2AK119ub1 levels at their promoters in LepR$^+$ BMSCs from 2-month-old *Bmi1*$^{\Delta LepR}$ mice (Figure 7A, B). Although their expression was only moderately activated in 2-month-old mice, it became evidently activated in 6-month-old mice (Figure 7C). RT-qPCR and 1 ChIP qPCR analyses confirmed the de-repression of *Nr2f1* and *Nr2f2* and reductions in H2AK119ub1 levels at their promoters in *Bmi1*-deficient LepR$^+$ BMSCs (Figures 7E, F). Nr2f2 directly and negatively regulates *Ppargc1a*, which encodes the metabolic regulator peroxisome proliferator-activated receptor γ coactivator 1-α (PGC-1α) [23]. Nr2f2 has been shown to bind to the *Ppargc1a* promoter at the promoter region 2 kb upstream of the transcriptional start site [23]. We also detected the binding of Nr2f2 to the *Ppargc1a* promoter (Figure 7G). PGC-1α has recently been reported to be downregulated with aging in SSCs, and its loss promotes the adipogenic differentiation of murine SSCs in BM [25]. Of note, *Ppargc1a* was significantly downregulated in *Bmi1*-deficient LepR$^+$ BMSCs with age (Figure 7D). These results suggest that *Nr2f2* and *Hox* family genes are among the candidate targets of Bmi1 responsible for the regulation of adipogenic differentiation in LepR$^+$ BMSCs.

Discussion

In the present study, we examined mice lacking Bmi1 in LepR$^+$ BMSCs, which include SSCs that are capable of differentiating into adipocytes in BM [7,11], and demonstrated that the *Bmi1* deletion promoted adipogenic changes in BM with age or after irradiation, resulting in reductions in BM cellularity and HSC numbers. We previously reported that *Bmi1* germ line knockout mice (*Bmi1*$^{\Delta/\Delta}$) had severely hypoplastic fatty marrow 8 weeks after birth [18]. The adipogenic changes observed in *Bmi1*$^{\Delta LepR}$ mice in the present study were milder than those in *Bmi1*$^{\Delta/\Delta}$ mice. This may have been because other mesenchymal cells compensated for defective LepR$^+$ cells in *Bmi1*$^{\Delta LepR}$ mice. HSC depletion was previously reported to be more severe when *Cxcl12* was conditionally deleted using *paired-related homeobox 1 (Prrx1)-Cre*, which is widely expressed in mesenchymal components, including LepR$^+$ stromal cells, osteoblasts, and other types of stromal cells, than *LepR-Cre* [26]. Indeed, the recently reported deletion of *Bmi1* using *Prrx1-Cre* induced more severe adipogenic changes in BM than the present study, with several different impacts on HSCs [27]. Together with this recent report, the present results clearly show that Bmi1 plays a critical role in the maintenance of LepR$^+$ BMSCs by restricting their adipogenic differentiation. Adipocyte-enriched yellow BM followed by hematopoietic failure is a hallmark of aging. Age-associated adipocyte accumulation is more evident in long bones than in flat bones. In this regard, *Bmi1*$^{\Delta LepR}$ mice recapitulated age-associated fatty changes in BM. Dysfunctions in or the reduced expression of BMI1 in BMSCs may, at least partially, account for the advanced fatty changes that occur in human BM with aging.

Irradiation and chemotherapy not only deplete HSCs but also disrupt their niche by destroying sinusoidal blood vessels and depleting stromal cells [28–31]. During niche regeneration, adipocytes become abundant in BM. Adipocyte progenitors, which are marked by adiponectin-CRE/ER and represent 5% of LepR$^+$ cells, proliferate after irradiation [32]. In the present study, the loss of Bmi1 clearly promoted adipogenic regeneration after irradiation, suggesting that Bmi1 restricts the differentiation of adipocyte progenitors. Although the accumulation of adipocytes in BM generally results in the depletion of HSCs, it differentially regulates HSC functions; sustained adipogenesis negatively regulates HSC frequency and hematopoietic regeneration, while transient adipogenesis after myeloablation in long bones promotes hematopoietic regeneration by secreting stem cell factor (SCF) [12,32]. Correspondingly, although *Bmi1*$^{\Delta LepR}$ mice had lower numbers of HSCs and progenitors because of the greater numbers of adipocytes in the long bones, residual HSCs retained an intact repopulation capacity. Because we used the *LepR-Cre* system, *Bmi1*$^{\Delta LepR}$ mice had more adipose mass and gained more

qPCR assays for H2AK119ub1 at the promoters of *Nr2f1* and *Nr2f2* in control and *Bmi1*$^{\Delta LepR}$ BM LepR$^+$ cells from 2-month-old male mice. The relative amounts of immunoprecipitated DNA are depicted as percentages of input DNA. Data are expressed as the mean ± SD of triplicate analyses. **(G)** ChIP qPCR assays for Nr2f2 binding to the *Ppargc1a* promoter in 3T3-L1 cells transduced with a pMYs empty vector virus and those transduced with a *3xFlag-Nr2f2* virus. ChIP assays were performed using an anti-Flag antibody. The relative amounts of immunoprecipitated DNA are depicted as percentages of input DNA. Data are expressed as the mean ± SD of triplicate analyses. $*p < 0.05$, $***p < 0.001$ by the Student's *t* test.

body weight than control mice with age. Enhanced adiposity may have had an impact on HSCs systemically to some extent in addition to the local effect of BM adipocytes.

Although promoters of as many as 11,908 genes were marked with H2AK119ub1 in the ChIP-seq analysis of LepR$^+$ stromal cells, only 3,581 genes showed reductions in H2AK119ub1 levels upon the *Bmi1* deletion. These results suggested the independent or redundant functions of other types of PRC1 in gene silencing. Traditionally, H2AK119ub1 was considered to be induced by Bmi1-containing PRC1, which is recruited to their target genes in a manner that is dependent on PRC2-mediated H3K27me3 modifications. On the other hand, noncanonical PRC1 complexes were recently identified that also catalyze H2AK119ub1 and are recruited independently of PRC2 [14,33,34]. The broad distribution of H2AK119ub1 and limited effects of the *Bmi1* deletion on H2AK119ub1 levels suggest that noncanonical PRC1 complexes contribute largely to the maintenance of gene expression in BM stromal cells. Nevertheless, the 3,581 genes exhibiting reductions in H2AK119ub1 levels in *Bmi1*-deficient stromal cells were considered to contain the critical targets of *Bmi1* in the regulation of adipogenesis. Of note, *Nr2f2* and *Hox* gene family members were found among the 559 genes, which exhibited reductions in H2AK119ub1 levels and the upregulation of gene expression upon the *Bmi1* deletion. *Nr2f2* and *Hox* gene family members have been implicated in adipogenesis [22–24]. Most of the genes in the HOX network are active in white as well as brown adipose tissues [22,24]. Nr2f2 is a family member of the steroid/thyroid nuclear receptor family of ligand-dependent transcription factors. The hemizygous *Nr2f2* deletion in mice perturbed adipocyte differentiation [23]. In line with the de-repression of *Nr2f2*, the expression of its direct and negative target gene *Ppargc1a*, which encodes Pgc-1α, was weaker in *Bmi1*-deficient cells than in control cells. PGC-1α is downregulated with aging in SSCs, and its loss promotes the adipogenic differentiation of murine SSCs in BM [25]. In this study, Bmi1 did not appear to directly target canonical adipogenesis regulator genes, such as *Ppargc1* and *Cebpa*. Therefore, it still remains obscure how Bmi1 restricts the adipogenic differentiation. In this regard, the role of *Nr2f2* and *Hox* gene family members in the maintenance of LepR$^+$ BMSCs should be further characterized.

Our present findings clearly showed that Bmi1 is essential for niche cells. Bmi1 was shown to restrict adipogenic differentiation of BMSCs to maintain the integrity of the HSC niche, as does its differentiation program in HSCs by repressing transcription of developmental regulator genes [18]. Various hematopoietic stresses not only damage hematopoietic cells but also induce adipogenic changes in BM, such as aging, irradiation, and exposure to anti-cancer agents. These hematopoietic stresses may compromise the function of Bmi1 in niche cells to activate the adipogenic differentiation program, thereby further promoting hematopoietic damage. It will be interesting to address this question in future studies and further elucidate the mechanisms that regulate the integrity of BM niche cells.

Acknowledgments

We thank Dr. Tatsuki Sugiyama and Dr. Takashi Nagasawa for their technical advice and Ola Mohammed Kamel Rizq for critically reviewing the manuscript. The supercomputing resource was provided by the Human Genome Center, Institute of Medical Science, University of Tokyo. This work was supported in part by Grants-in-Aid for Scientific Research (No. 18K19555) and Scientific Research on Innovative Areas “Stem Cell Aging and Disease” (No. 26115002) from MEXT, Japan.

References

1. Kunisaki Y, Bruns I, Scheiermann C, et al. Arteriolar niches maintain haematopoietic stem cell quiescence. Nature. 2013;502:637–643.
2. Acar M, Kocherlakota KS, Murphy MM, et al. Deep imaging of bone marrow shows non-dividing stem cells are mainly perisinusoidal. Nature. 2015;526:126–130.
3. Chen JY, Miyanishi M, Wang SK, et al. Hoxb5 marks long-term haematopoietic stem cells and reveals a homogenous perivascular niche. Nature. 2016;530:223–227.
4. Crane GM, Jeffery E, Morrison SJ. Adult haematopoietic stem cell niches. Nat Rev Immunol. 2017;17:573–590.
5. Wei Q, Frenette PS. Niches for hematopoietic stem cells and their progeny. Immunity. 2018;48:632–648.
6. Sugiyama T, Kohara H, Noda M, Nagasawa T. Maintenance of the hematopoietic stem cell pool by CXCL12–CXCR4 chemokine signaling in bone marrow stromal cell niches. Immunity. 2006;25:977–988.
7. Zhou BO, Yue R, Murphy MM, et al. Leptin-receptor-expressing mesenchymal stromal cells represent the main source of bone formed by adult bone marrow. Cell Stem Cell. 2014;15:154–168.
8. Ding L, Saunders TL, Enikolopov G, Morrison SJ. Endothelial and perivascular cells maintain haematopoietic stem cells. Nature. 2012;481:457–462.
9. Asada N, Kunisaki Y, Pierce H, et al. Differential cytokine contributions of perivascular haematopoietic stem cell niches. Nat Cell Biol. 2017;19:214–223.
10. Ding L, Morrison SJ. Haematopoietic stem cells and early lymphoid progenitors occupy distinct bone marrow niches. Nature. 2013;495:231–235.
11. Yue R, Zhou BO, Shimada IS, et al. Leptin receptor promotes adipogenesis and reduces osteogenesis by regulating mesenchymal stromal cells in adult bone marrow. Cell Stem Cell. 2016;18:782–796.
12. Naveiras O, Nardi V, Wenzel PL, et al. Bone-marrow adipocytes as negative regulators of the haematopoietic microenvironment. Nature. 2009;460:259–263.
13. Ambrosi TH, Scialdone A, Graja A, et al. Adipocyte accumulation in the bone marrow during obesity and aging impairs stem cell-based hematopoietic and bone regeneration. Cell Stem Cell. 2017;20:771–784.

14. Blackledge NP, Rose NR, Klose RJ. Targeting Polycomb systems to regulate gene expression: modifications to a complex story. Nat Rev Mol Cell Biol. 2015;16:643–649.
15. Iwama A. Polycomb repressive complexes in hematological malignancies. Blood. 2017;130:23–29.
16. Park IK, Qian D, Kiel M, et al. Bmi-1 is required for maintenance of adult self-renewing haematopoietic stem cells. Nature. 2003;423:302–305.
17. Iwama A, Oguro H, Negishi M, et al. Enhanced self-renewal of hematopoietic stem cells mediated by the polycomb gene product, Bmi-1. Immunity. 2004;21:843–851.
18. Oguro H, Iwama A, Morita Y, et al. Differential impact of *Ink4a* and *Arf* on hematopoietic stem cells and their bone marrow microenvironment in Bmi1-deficient mice. J Exp Med. 2006;203:2247–2253.
19. Omatsu Y, Seike M, Sugiyama T, et al. Foxc1 is a critical regulator of haematopoietic stem/progenitor cell niche formation. Nature. 2014;508:536–540.
20. Baryawno N, Przybylski D, Kowalczyk MS, et al. A cellular taxonomy of the bone marrow stroma in homeostasis and leukemia. Cell. 2019;177:1915–1932.
21. Green H, Kehinde O. An established preadipose cell line and its differentiation in culture. II. Factors affecting the adipose conversion. Cell. 1975;5:19–27.
22. Cantile M, Procino A, D'Armiento M, et al. HOX gene network is involved in the transcriptional regulation of in vivo human adipogenesis. J Cell Physiol. 2003;194:225–236.
23. Li L, Xie X, Qin J, et al. The nuclear orphan receptor COUP-TFII plays an essential role in adipogenesis, glucose homeostasis, and energy metabolism. Cell Metab. 2009;9:77–87.
24. Singh S, Rajput YS, Barui AK, et al. Fat accumulation in differentiated brown adipocytes is linked with expression of Hox genes. Gene Expr Patterns. 2016;20:99–105.
25. Yu B, Huo L, Liu Y, et al. PGC-1α controls skeletal stem cell fate and bone–fat balance in osteoporosis and skeletal aging by inducing TAZ. Cell Stem Cell. 2018;23:193–209.
26. Greenbaum A, Hsu YM, Day RB, et al. CXCL12 in early mesenchymal progenitors is required for haematopoietic stem-cell maintenance. Nature. 2013;495:227–230.
27. Hu T, Kitano A, Luu V, Dawson B, Hoegenauer KA, Lee BH, Nakada D. Bmi1 suppresses adipogenesis in the hematopoietic stem cell niche. Stem Cell Rep. 2019 Jun 12. https://doi.org/10.1016/j.stemcr.2019.05.027. [Epub ahead of print].
28. Kopp HG, Avecilla ST, Hooper AT, et al. Tie2 activation contributes to hemangiogenic regeneration after myelosuppression. Blood. 2005;106:505–513.
29. Li XM, Hu Z, Jorgenson ML, et al. Bone marrow sinusoidal endothelial cells undergo nonapoptotic cell death and are replaced by proliferating sinusoidal cells in situ to maintain the vascular niche following lethal irradiation. Exp Hematol. 2008;36:1143–1156.
30. Hooper AT, Butler JM, Nolan DJ, et al. Engraftment and reconstitution of hematopoiesis is dependent on VEGFR2-mediated regeneration of sinusoidal endothelial cells. Cell Stem Cell. 2009;4:263–274.
31. Si S, Nakajima-Takagi Y, Iga T, et al. Hematopoietic insults damage bone marrow niche by activating p53 in vascular endothelial cells. Exp Hematol. 2018;63:41–51.
32. Zhou BO, Yu H, Yue R, et al. Bone marrow adipocytes promote the regeneration of stem cells and haematopoiesis by secreting SCF. Nat Cell Biol. 2017;19:891–903.
33. Kondo T, Ito S, Koseki H. Polycomb in transcriptional phase transition of developmental genes. Trends Biochem Sci. 2016;41:9–19.
34. Isshiki Y, Iwama A. Emerging role of non-canonical polycomb repressive complexes in normal and malignant hematopoiesis. Exp Hematol. 2018;68:10–14.